A Parameterized Geometric Model of the Oral Tract for Aero acoustic Simulation of Fricatives

Julien Cisonni, Kazunori Nozaki, Annemie Van Hirtum, and Shigeo Wada

Abstract— **The sound generated during the production of the sibilant [s] results from the impact of a turbulent jet on the incisors. Physical modeling of this phenomenon depends on the characterization of the turbulent flow within the vocal tract and of the acoustic sources resulting from the presence of an obstacle in the path of the flow. The properties of the flow-induced noise strongly depend on several geometric parameters of which the influence has to be determined. In this paper, a simplified geometric model of the oral tract is used to carry out a numerical study of the flow-induced noise generated by a turbulent flow. It is shown from the numerical simulations performed that the modification of the configuration of the geometric model influences the behavior of the turbulent flow and hence the spectral properties and the level of the flow-induced noise generated.**

Index Terms—**Aero acoustic modeling, fricatives, Large-Eddy Simulation, sibilant [s].**

I. Introduction

Fricatives are unvoiced sounds of speech which are produced by the development of a jet of air in the oral tract. The interaction of this jet with different components of the vocal tract, also called articulators, as the lips, the teeth or the tongue, generates acoustic sources at the origin of the different fricative sounds. The sibilant [s] results from the impact of a turbulent jet, created by a narrow channel formed by the tongue, on the incisors. Experimental studies [1] characterized the main mechanisms and in particular the strong acoustic source resulting from the presence of an obstacle in a turbulent flow. [2] investigated the influence of the location of the sibilant groove on the sound produced. Despite the variability in the place of articulation, the resulting sounds can be perceived as a [s] by listeners. [3] carried out an analysis of spectral parameters of fricatives produced by adults and developing children and showed an increase in the acoustic distinction between [s] and the other sounds as the age of speaker increased. Moreover, [4] pointed out the increase in the high frequency spectral energy of sibilant produced by speakers wearing dentures.

The modeling of the turbulent flow within the cavities and the constrictions of the vocal tract is essential to characterize the acoustic sources of the fricatives. From predictions obtained with a Large-Eddy Simulation model and a simplified description of the vocal tract, [5] suggest that aeroacoustic models of the turbulence in fricatives with a small number of geometric parameters can be developed but also that using very simplified description of turbulent jet doesn't seem to be relevant for the modeling of fricatives. Moreover [6] strongly suggests that the interaction of the turbulent jet with the oral tract geometry is generating the noise from the pressure forces induced on the vocal tract walls. Thus, the discontinuities in the vocal tract shape appear to have a key role in the fricative sound production. Complete aeroacoustic models of the sibilant [s] production using simplified [7] or realistic 2-D [8] and 3-D [9] geometries of the vocal tract and the teeth were proposed, but the influence of geometric parameters on the properties of the sound generated was not clearly determined. Experimental in-vivo [10] and in-vitro [11] studies showed that small variations of the position of the tongue and the incisors can lead to significant changes in the spectral characteristics of the sound generated and therefore in the type of speech sound produced.

Thus, a systematic analysis of the influence of different geometric parameters on the properties of the sound generated, from numerical aeroacoustic simulation, appears to be a necessary phase in the development of a physical model of fricatives. Even if simplified geometrical models of the vocal tract remain unable to predict unvoiced sounds of speech [12], they are still useful to analyze the physics involved in the production of these sounds. The use of a simplified vocal tract/teeth obstacle allows focusing the study on one particular phenomenon which can be isolated. Moreover, it allows carrying out in-vitro experiments using the same geometry [13] which can be compared to results obtained from numerical simulations in order to provide an experimental validation of the physical modeling [14].

In this paper, a simplified and parameterized geometric model based on the configuration of the oral tract during the sibilant [s] production is presented. This model is used to perform flow simulations in order to analyze the sound generation due to the turbulent airflow circulating in this simplified geometry, relevant to the oral tract. The sound source involved in the sibilant [s] production is indeed strongly linked to the separation of the flow and the

Manuscript received September 16, 2011; revised October 22, 2011.This work has been supported by Strategic International Cooperative Program, Japan Science and Technology Agency (JST) and ANR "Petaflow" - CSD1-ANR-09- BLAN-0376-01.

J. Cisonni is with the Center for Advanced Medical Engineering and Informatics, Osaka University, 1-3 Machikaneyama, Toyonaka, Osaka 560-8531, Japan (e-mail: julien.cisonni@gmx.com).

K. Nozaki is with the Department of Mechanical Science & Bioengineering, Graduate School of Engineering Science, Osaka University, 1-3 Machikaneyama, Toyonaka, Osaka 560-8531, Japan (e-mail: nozaki@dentgrid.org).

A. Van Hirtum is with GIPSA-lab, UMR CNRS 5216, Grenoble University, 961 rue de la Houille Blanche, BP 46, 38402 Grenoble Cedex, France (e-mail: annemie.vanhirtum@gipsa-lab.grenoble-inp.fr).

S. Wada is with the Department of Mechanical Science & Bioengineering, Graduate School of Engineering Science, Osaka University, 1-3 Machikaneyama, Toyonaka, Osaka 560-8531, Japan (e-mail: shigeo@me.es.osaka-u.ac.jp).

formation of a jet which interacts with the teeth. From three geometric configurations, the influence of geometric parameters which affect the properties and the position relatively to the teeth of the turbulent jet, and hence, the spectral properties and the level of the flow-induced noise produced is discussed.

II. Numerical Simulations

Numerical flow simulations were carried out using the simplified geometric model of the vocal tract described in Section II.A. The Large-Eddy Simulation method for incompressible flow was used to simulate the turbulent flow within this model. The conditions and the parameters used for this modeling are given in Section II.B and Section II.C. The flow-induced noise sources were derived from the results of the flow simulations as described in Section II.D.

A. Geometric Model

Simulations were implemented using the geometry described in Fig. 1 and Fig. 2, and in Table I and Table II. The shape and the sizes of the geometric model are relevant to the configuration of the oral tract during the production of the sibilant [s] [9]. This geometry is mainly characterized by two obstacles representing the upper and lower teeth, and in particular the incisors. Upstream of these obstacles, the geometry is defined by two cavities and one constriction which correspond to the position of the tongue in the mouth. Downstream of the obstacles, the geometry is defined by a third cavity which corresponds to the gap between the teeth and the lips and leads to the exit of the vocal tract to the free field, defined by a rectangular box.

In this study, three configurations were defined by changing two parameters, as reported in Table II:

- The first configuration (*case I*) is the reference configuration where the geometry is completely symmetric over (y=0) plane.
- In the second configuration (*case II*), the center of the duct upstream of the second cavity is shifted by a height of 0.5 mm from the center of the second cavity. With this configuration, the geometry is asymmetric over (y=0) plane.
- In the third configuration (*case III*), the center of the constriction formed by the teeth-shaped obstacles is shifted by a height of 0.75 mm from the center of the second and third cavities. With this configuration, the geometry is asymmetric over (y=0) plane.

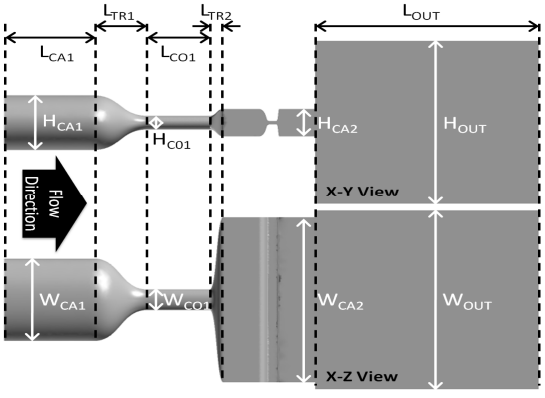

Fig. 1. Description of the geometric model in (x,y) and (x,z) planes.

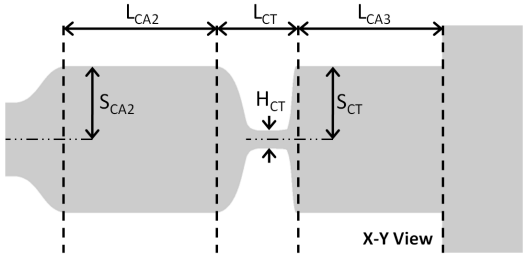

Fig. 2. Close-up description of the geometric model around the teeth constriction in (x,y) plane.

TABLE I: Parameters of the Geometric Model

Quantity	Symbol	Value (mm)
Cavity 1 Length	L_{CA1}	10
Transition 1 Length	L_{TR1}	6
Constriction 1 Length	L_{CO1}	7
Transition 2 Length	L_{TR2}	1.5
Cavity 2 Length	L_{CA2}	4
Teeth Constriction Length	L_{CT}	2.25
Cavity 3 Length	L_{CA3}	4
Free Field Length	L_{OUT}	25
Cavity 1 Width	W_{CA1}	12
Constriction 1 Width	W_{CO1}	3
Cavity 2 Width	W_{CA2}	24
Free Field Width	W_{OUT}	26
Cavity 1 Height	H_{CA1}	8
Constriction 1 Height	H_{CO1}	2
Cavity 2 Height	H_{CA2}	4
Teeth Constriction Height	H_{CT}	0.5
Free Field Height	H_{OUT}	24
Cavity 2 Shift	S_{CA2}	See Table II
Teeth Constriction Shift	S_{CT}	See Table II

TABLE II: Parameters Corresponding to the Cases Considered

Shifted Part	Case I	Case II	Case III
Cavity 2 - S_{CA2}	2 mm	*1.5 mm*	2 mm
Teeth Constriction - S_{CT}	2 mm	2 mm	*2.75 mm*

B. Meshing and Boundary Conditions

The spatial discretization of the whole flow domain was carried out using *SC*-Tetra *v8 (Cradle Co., Ltd.)*. An unstructured mesh was defined by using tetrahedral finite volumes. Smaller volumes were defined near the walls and in the regions where turbulent jets are expected whereas it was coarser in the body of the flow and near the boundaries of the free field. Besides, prism volumes were inserted in the region near the walls to take into account the boundary layer effects. In the different cases considered, the total number of elements was about 5,000,000.

The boundary conditions were defined by specifying a uniform velocity profile at the duct entrance (inlet) and a static pressure equal to 0 at the boundaries of the free field (outlet). The inlet velocity was set to 1.875 $m \cdot s^{-1}$ to obtain a typical Reynolds number value of 4000 at the exit of the first constriction. Except at the inlet and outlet, the no-slip wall condition was specified at all the boundaries of the channel. The different boundary conditions are indicated on Fig. 3.

C. Flow Modeling

The flow modeling was carried out using the Large-Eddy Simulation (L.E.S.) method [15] for incompressible and isothermal flow implemented in *SC-Tetra v8*. The

subgrid-scale eddy viscosity was computed using dynamic Smagorinsky model [16] and the filter width was derived automatically from the mesh size. To ensure the numerical stability of the model, a 1μs time step was used for all the simulations. For each case, 50,000 time steps were simulated to generate 50 ms of flow motion. The flow simulations were performed using a 16 cores PC cluster allowing the computation of 1,000 time steps of the model in 1 hour.

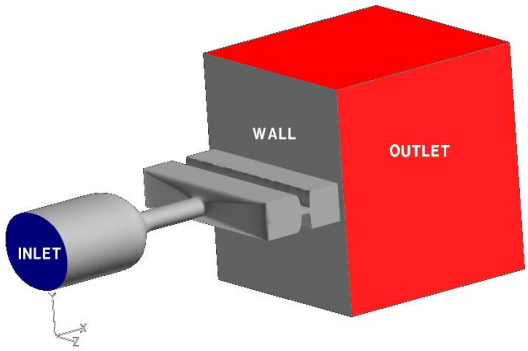

Fig. 3. 3-D view of the geometric model with the different boundary conditions.

D. Flow-induced noise sources

The presence of the teeth as an obstacle in the flow is assumed to be a strong acoustic source [1] and the interactions of the flow with the surrounding walls are assumed to mostly produce sound [6]. Accounting for these assumptions, it can be considered that the main noise source is strongly linked to the fluctuations of the pressure forces exerted on the walls of the vocal tract model. Thus, the flow-induced noise level as well as its spectral properties can be estimated from the surface pressure predicted by the flow simulation. In order to analyze the influence of the considered parameters on the properties of the flow-induced noise source, the values $\tilde{F}$ of the time derivative of the pressure force obtained for the *case I*, *case II* and *case III* are compared. This quantity is defined as:

$$\tilde{F}(t) = \int_S \frac{dp(t)}{dt} ds \tag{1}$$

where p is the pressure on the vocal tract walls surface S. In the following, the comparison of $\tilde{F}$ is made in the frequency domain so that:

$$\tilde{F}_{dB}(\omega) = 20 \cdot \log_{10}\left(\tilde{F}(\omega)\right) \tag{2}$$

Even if the power of the sound generated by the vorticity of the flow (quadrupole source) is expected to be weak compared to the power of the sound generated by the interaction of the turbulent flow with the walls (dipole source) due to the low Mach number characterizing the flow in this study [17], it seems interesting to estimate this secondary source and in particular to determine the regions where it is stronger and where it might be not negligible. Thus, in the following, the flow-induced noise sources due to the vorticity of the flow, obtained for *case I*, *case II* and *case III*, are compared. This comparision is based on the *Powell-Howe* source term Q_{PH} defined as:

$$Q_{PH} = \rho \, div\left(\vec{\omega} \times \vec{u}\right) \tag{3}$$

where ρ is the density of air, $\vec{u}$ is the velocity vector and $\vec{\omega}$ is the vorticity vector defined as:

$$\vec{\omega} = curl\,(\vec{u}) \tag{4}$$

III. Simulation Results and Discussion

For each case considered, the developed flow field was simulated for 50 ms. In this section, the results presented are time-averaged over this time range of 50 ms.

(a)

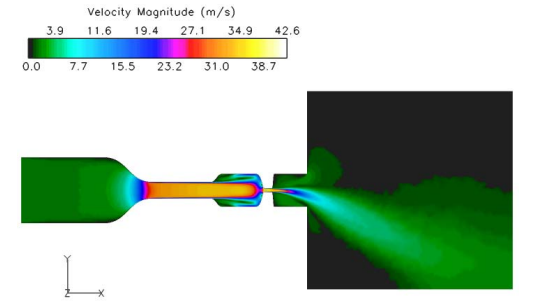

(b)

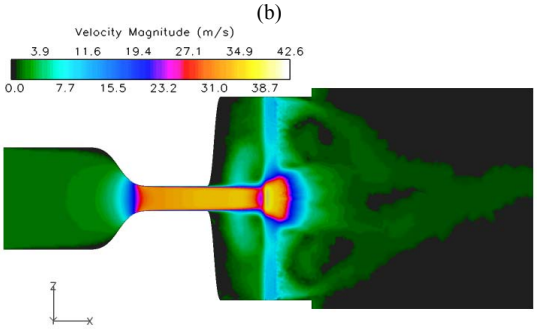

Fig. 4. Average velocity magnitude field in (x,y,z=0) plane (a) and in (x,y=0,z) plane (b) for *case I*.

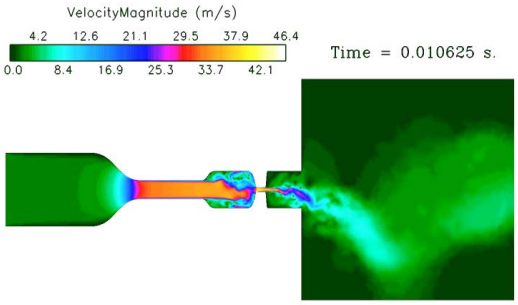

Fig. 5. Snapshot of the velocity magnitude field in (x,y,z=0) plane for *case I*.

(a)

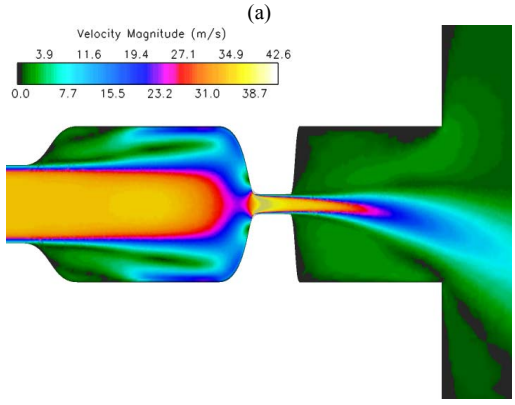

(b)

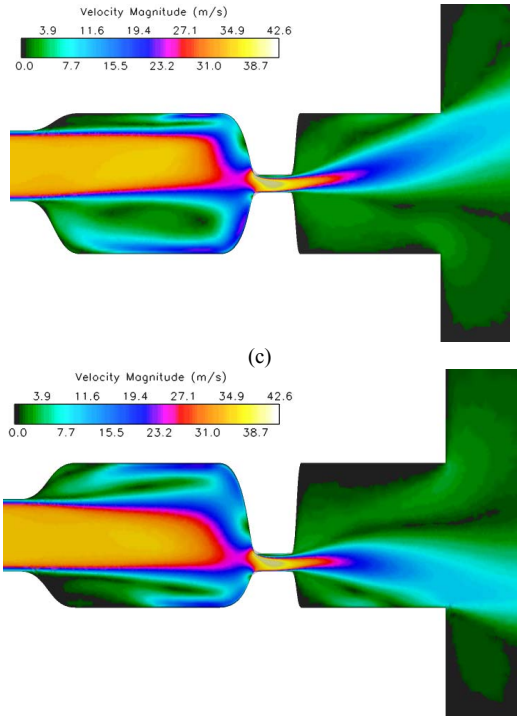

Fig. 6. Close-up view of the average velocity magnitude field in (x,y,z=0) plane for *case I* (a), *case II* (b) and *case III* (c).

A. Velocity Field

Fig. 4 presents the velocity magnitude field obtained for *case I* in (x,y,z=0) plane and (x,y=0,z) plane. It can be observed from this figure that a first jet is formed at the exit of the first constriction in the second cavity representing the space between the tongue and the teeth. This jet hits the teeth-shaped obstacles and a flow recirculation region appears in the second cavity. The flow accelerates at the entrance of the constriction formed by the teeth-shaped obstacles and a second turbulent jet is formed at the exit of this constriction in the third cavity and downstream in the free field. The average velocity in the region upstream of the teeth constriction is lower than in the core of the first jet and than in the teeth constriction. Indeed, the first jet oscillates and the presence of the obstacles in its path creates a back-flow which tends to decrease the average value of the velocity magnitude. The length of the core of the second jet formed downstream of the obstacles is also affected by the turbulent flow upstream of the obstacles. Indeed, the flow around the teeth-shaped obstacles and in particular in the second jet is very unstable, as shown in Fig. 5, so that the average jet width increases and the average velocity decreases rapidly downstream of the teeth constriction.

The comparison, presented in Fig. 6, of the average velocity magnitude fields obtained for the three cases considered shows that for *case I*, the average flow is symmetric over (y=0) plane except in the region downstream the teeth-shaped obstacles and in the free field. Indeed, the geometric configuration corresponding to *case I* is symmetric over (y=0) plane but the instability of the jet implies that one particular side is favored so that the average jet tends to be on that side (Coanda effect). For *case II* and *case III*, the geometric configuration is asymmetric so that the average flow is also asymmetric. Thus, a stronger acceleration of the flow occurs on the upper side of the teeth constriction entrance.

B. Pressure Field

The impact of the jet formed in the second cavity on the teeth-shaped obstacles produces a high pressure on the upstream face of the teeth-shaped obstacles whereas the acceleration of the flow at the entrance of the teeth constriction produces a low pressure on the walls at the tip of the teeth-shaped obstacles, as shown in Fig. 7. Moreover, the pressure within the teeth constriction becomes negative. Thus, in the region around the teeth constriction entrance, the pressure gradient (and the pressure laplacian) on the surface of the teeth-shaped obstacles is very high in comparison to the other region of the wall surfaces, so that this region corresponds to the one where the sound is likely to be mainly generated.

As for the average velocity magnitude field, the average pressure field is symmetric over (y=0) plane for *case I* and asymmetric for *case II* and *case III*. For the two asymmetric configurations, the maximum pressure is slightly higher on the upstream face of the teeth-shaped obstacles than for *case I* but the minimum pressure within the teeth constriction is also slightly higher than for *case I*. Regarding the pressure fluctuations, the Root-Mean-Square pressure is higher for *case II* and *case III* than for *case I*. Since the pressure on the walls surface is directly linked to the power of the sound source, the noise generated with the asymmetric configuration will be higher.

C. Flow-induced Noise Sources

The analysis of the sound sources linked to the vorticity of the flow gives an indication of the location of the stronger quadrupole sources within the flow. Fig. 8 presents the distribution of the *Powell-Howe* sound source in the region around the teeth-shaped obstacles in (x,y,z=0) plane for the three geometric configurations considered. This figure shows that the maximum of the *Powell-Howe* source term is located in the region of the entrance of the teeth constriction which corresponds to the region where a strong acceleration of the flow occurs and where the pressure gradient is the highest. Moreover, it can be noticed that the sound sources are mainly concentrated in the boundary layer of the flow near the walls of the tip of the teeth-shaped obstacles. Since the *Powell-Howe* source term is directly derived from the velocity (see (3)), the asymmetry of the flow velocity in this region leads to asymmetric distributions of the *Powell-Howe* source term for the *case II* and *case III*. Moreover, the sources are stronger for the two asymmetric configurations ($max(Q_{PH})\approx10^{12}$) than for *case I* ($max(Q_{PH})\approx10^{11}$). Within and downstream the teeth constriction, the strength of the *Powell-Howe* source term is more moderate. The sound sources remain confined in the boundary layer of the flow within the constriction and in the mixing layer of the jet farther downstream. These regions correspond to the ones where the turbulence intensity of the flow is the highest.

As mentionned in Section II.D, the interactions of the flow with the surrounding walls are expected to be predominant in the production of sound. The dipole sound

Sources are associated with the pressure fluctuations on the surface of the walls. Thus the spectral properties of the dipole sound sources can be estimated from the analysis in the frequency domain of the fluctuating pressure force

exerted on the walls of the geometric model. Fig. 9 presents a comparison of the spectra of the pressure force fluctuations obtained for the three configurations considered. This figure shows that the different spectra have similar features and are characterized by two disctint regions, respectively below 8kHz and above 10kHz. Below 8kHz, the change of geometric configuration seems to have a limited influence on the spectral properties of the wall pressure fluctuations since the spectra obtained for the three cases present comparable levels and some coincident peaks. Between 8kHz and 10kHz

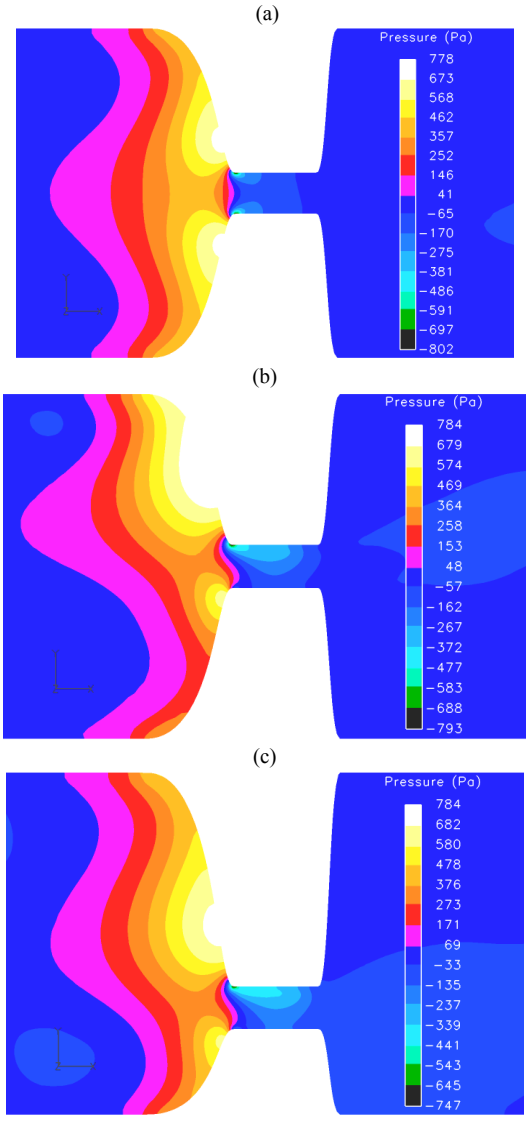

Fig. 7. Close-up view of the average pressure field in (x,y,z=0) plane for *case I* (a), *case II* (b) and *case III* (c).

,

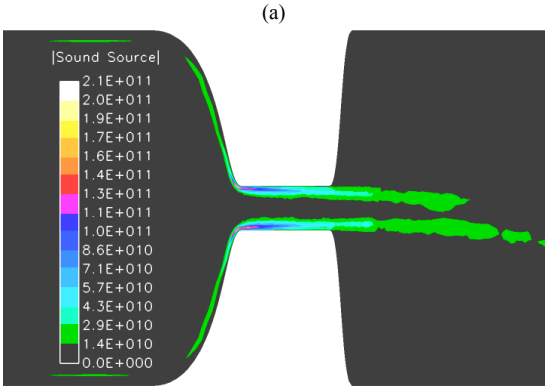

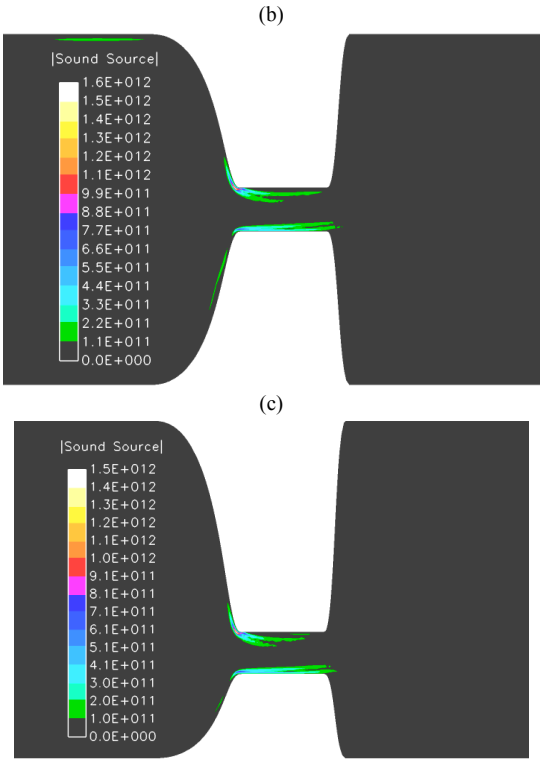

Fig. 8. Close-up view of the average *Powell-Howe* sound source field in (x,y,z=0) plane for *case I* (a), *case II* (b) and *case III* (c).

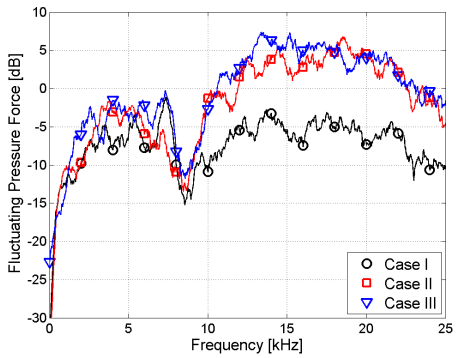

Fig. 9. Spectra of the fluctuating pressure force exerted on the walls surface for the three cases considered.

a drop of the magnitude of the fluctuating pressure force can be observed for the three configurations. Above 10kHz, the spectra present some coincident peaks but the level is substantially higher, with a difference of about 10dB, for the two asymmetric geometric configurations than for *case I*. Thus, asymmetry in the configuration of the geometric model has a more significant influence on the wall pressure fluctuations for higher frequencies, above 10kHz. For *case I*, the geometry is symmetric over the plane (y=0) and the first turbulent jet is centered in the second cavity as well as the constriction formed by the teeth-shaped obstacles. For *case II* and *case III*, the geometry is asymmetric over the plane (y=0) so that the impact of the first jet formed in the second cavity on the surface of the obstacles is more direct and induces stronger acoustic sources.

IV. Conclusion

The geometric model presented allows performing numerical aeroacoustic simulations aiming the characterization of the sound generation during the

production of fricatives and in particular the sibilant [s]. Since the geometry is simplified and parameterized, it can be considered as a generic oral tract model which can be used to determine the influence of different geometric parameters on the properties of the flow and of the sound produced.

This study shows the importance of the flow behavior upstream of the teeth. Indeed, the position of the turbulent jet within the oral tract relatively to the teeth influences the properties of the turbulent jet downstream of the teeth and the strength of the resulting acoustic sources, in particular at high frequencies.

However, deeper analyses of the flow properties are required, as well as a more sophisticated acoustic modeling (using Computational AeroAcoustic methods) in order to obtain a better characterization of the sound produced by a turbulent flow circulating in this oral tract model.

REFERENCES

[1] C. H. Shadle, "The acoustics of fricative consonants," Ph.D. dissertation, Massachusetts Institute of Technology, Cambridge, MA, 1985.

[2] S. G. Fletcher and D. G. Newman, "[s] and [/] as a function of linguapalatal contact place and sibilant groove width," *J. Acoust. Soc. Am.*, vol. 89, pp. 850–858, 1991.

[3] S. L. Nissen and R. A. Fox, "Acoustic and spectral characteristics of young childrens fricative productions: A developmental perspective," J. Acoust. Soc. Am., vol. 118, pp. 2570–2578, 2005.

[4] J. C. Catford, *Fundamental problems in phonetics*, Indiana University Press, Bloomington, IN, USA, 1977.

[5] G. Ramsay and C. Shadle, "The influence of geometry on the initiation of turbulence in the vocal tract during the production of fricatives," *in Proc. 7th International Seminar on Speech Production (ISSP)*, 2006, pp. 581–588.

[6] M. H. Krane, "Aeroacoustic production of low-frequency unvoiced speech sounds," J. Acoust. Soc. Am., vol. 118 (1), pp. 410–427, 2005.

[7] M. Howe and R. McGowan, "Aeroacoustics of [s]," *Proc. R. Soc. A*, vol. 461, pp. 1005–1028, 2005.

[8] P. Anderson, S. Green, and S. Fels, "Modeling fluid flow in the airway using CFD with a focus on fricative acoustics,", *in Proc. 1st* International *Workshop on Dynamic Modeling of the Oral, Pharyngeal and Laryngeal Complex for Biomedical Applications (OPAL-2009)*, 2009, pp. 146–154.

[9] K. Nozaki, "Numerical Simulation of Sibilant [s] Using the Real Geometry of a Human Vocal Tract," *in Proc. High Performance* Computing *on Vector Systems, Springer Berlin Heidelberg*, 2010, pp. 137-148.

[10] C. Runte, M. Lawerino, D. Dirksen, F. Bollmann, A. Lamprecht-Dinnesen, and E. Seifert, "The influence of maxillary central incisor position in complete dentures on /s/ sound production," *The Journal of Prosthetic Dentistry*,vol. 85 (5), pp. 485–495, 2001.

[11] C. H. Shadle, M. Berezina, M. Proctor and K. Iskarous, "Mechanical models of fricatives based on MRI-derived vocal tract shapes," *in Proc. 8th* International *Seminar on Speech Production (ISSP)*, 2008, pp. 417–420.

[12] C. H. Shadle, "The effect of geometry on source mechanisms 1 of fricative consonants," *J. Phon.*, vol. 19, pp. 409–424, 1991.

[13] A. Van Hirtum, X. Grandchamp, X. Pelorson, K. Nozaki and S. Shimojo, "Large Eddy Simulation and 'in-vitro' experimental validation of flow around a teeth-shaped obstacle," *Int. J. of Applied Mechanics*, vol. 2, pp. 265–279, 2010.

[14] A. Van Hirtum, X. Pelorson, O. Estienne and H. Bailliet, "Experimental validation of flow models for a rigid vocal tract replica," *J. Acoust. Soc. Am.*, Accepted.

[15] P. Sagaut, *Large Eddy Simulation for incompressible flows: an* introduction, Springer, Berlin, Germany, 2005.

[16] M. Germano, U. Piomelli, P. Moin, and W. H. Cabot, "A dynamic subgridscale eddy-viscosity model," Physics of Fluids A, vol. 3 (7), pp. 1760-1765, 1991.

[17] M. E. Goldstein, *Aeroacoustics*, McGraw Hill, New York, NY, USA, 1976.